Accepted Manuscript

A label-free genetic biosensor for diabetes based on AuNPs decorated ITO with electrochemiluminescent signaling

Suyan Zhai, Chen Fang, Jilin Yan, Qun Zhao, Yifeng Tu

PII: S0003-2670(17)30693-1

DOI: 10.1016/j.aca.2017.05.028

Reference: ACA 235238

To appear in: *Analytica Chimica Acta*

Received Date: 25 February 2017

Revised Date: 17 May 2017

Accepted Date: 19 May 2017

Please cite this article as: S. Zhai, C. Fang, J. Yan, Q. Zhao, Y. Tu, A label-free genetic biosensor for diabetes based on AuNPs decorated ITO with electrochemiluminescent signaling, *Analytica Chimica Acta* (2017), doi: 10.1016/j.aca.2017.05.028.

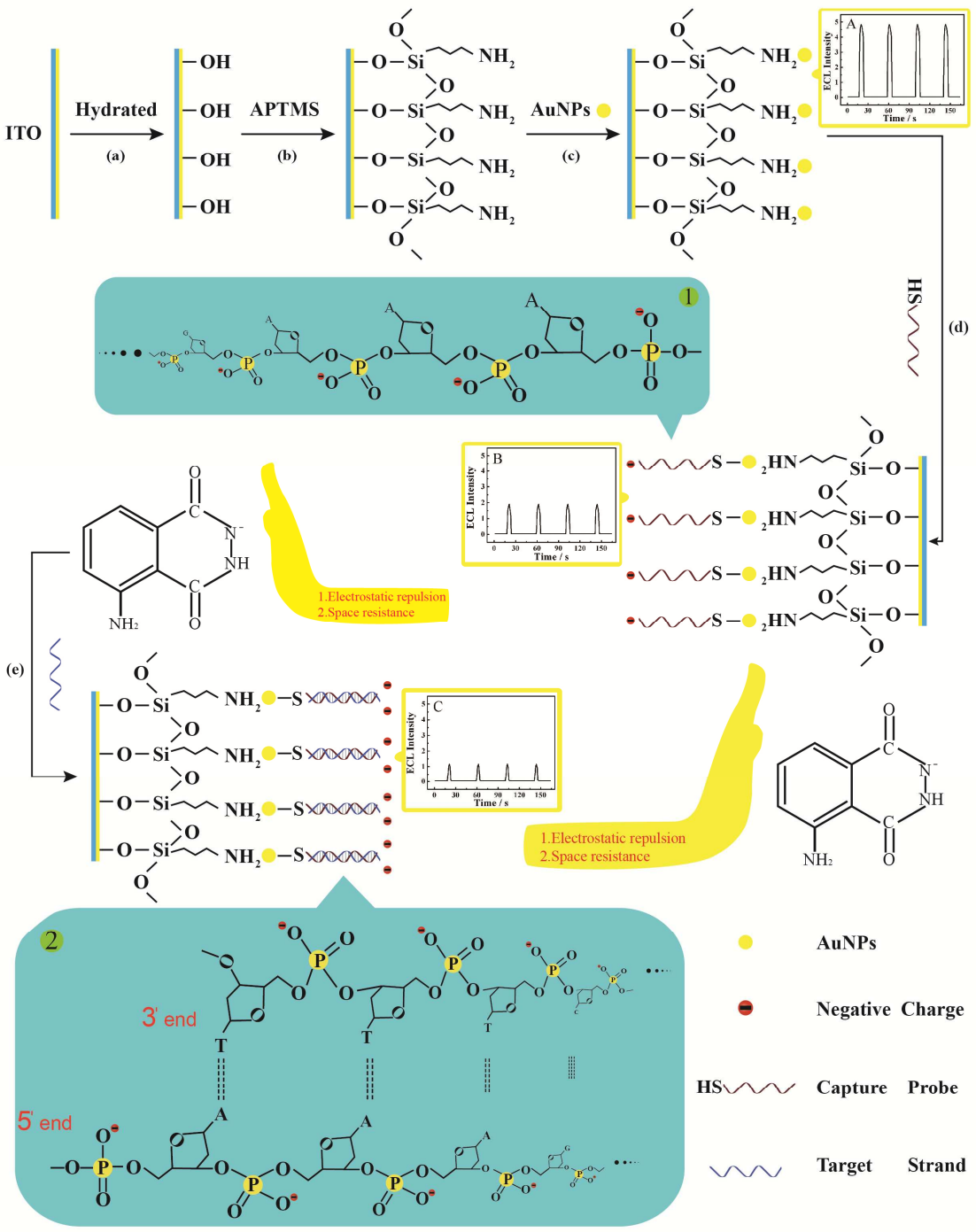
ITO
Hydrated
(a)
APTMS
(b)
AuNPs
(c)
(d)
(e)
1.Electrostatic repulsion
2.Space resistance
1.Electrostatic repulsion
2.Space resistance
3' end
5' end
AuNPs
Negative Charge
Capture Probe
Target Strand

A label-free genetic biosensor for diabetes based on AuNPs decorated ITO with electrochemiluminescent signaling

Suyan Zhai[1†], Chen Fang[1, 2†], Jilin Yan[1], Qun Zhao[1, 3]* and Yifeng Tu[1]*

1. Institute of Analytical Chemistry, Dushu Lake Campus, Soochow University, Industrial Park, Suzhou, 215123, P. R. China

2. Second Affiliated Hospital, Soochow University, Suzhou, 215004, P. R. China

3. College of Chemistry and Chemical Engineering, Nantong University, Nantong, 226019, P. R. China

†: Joint first author

*: To whom the correspondence should be addressed. Prof. PhD. Tu Yifeng, Tel: 86-13812768378, E-mail: tuyf@suda.edu.cn; PhD. Zhao Qun, 25315885@qq.com

Abstract

The variation of I27L gene closely relates to increasing risk of type 2 diabetes, thus it is greatly significant to develop various methods for its identification or monitoring. We report here a novel label-free electrochemiluminescent (ECL) biosensor for simple and effective determination of I27L gene based on Au nanoparticles functionalized ITO electrode. The ECL technique is employed to monitor the hybridization of DNA strands by measuring the changes of its intensity. Here, the ECL signal was quenched by blocked access of probe (luminol anion) owing to the electrostatic repulsion of negatively charged sensor surface and the space resistance. The quantification of target strand can be directly realized by calibrating the quenched ECL signal toward its logarithm concentration in good linearity within the range from 1.0×10^{-11} to 1.0×10^{-7} M and a detection limit of 8.1×10^{-12} M. In addition, the biosensor exhibited good stability, excellent reproducibility and outstanding selectivity against one-base mismatched strand. What's more, the simple, low-cost, sensitive device could be easily miniaturized, makes it as an attractive candidate for integrating into portable platforms for point-of-care molecular diagnostics.

Keywords: Diabetes; Genovariation; I27L; Electrochemiluminescence; Luminol; Au nanoparticles

1. Introduction

Diabetes is caused by complex interplays including genetic or environmental factors [1]. On account of the statistics of International Diabetes Federation (IDF), there are 415 million of persons living with diabetes in 2015, and will rise to 642 million by 2040 if we do nothing. Especially distressing matters are a 5 millions of mortality and greater than 673 billions US$ of the healthcare spending per year by the end of 2015 [2]. Diabetes and its complications not only cause serious injury to physical and mental health of patients, but also make a heavy burden to themselves, their families and society. Now, it has turned into one of the greatest global health problems of the 21st century, including about 110 millions crowd of diabetics in China [2, 3].

Type 2 diabetes mellitus (T2DM) is the most prevalent form of diabetes, accounting for >90% of cases [4]. Chiu *et al* have indicated that the HNF1α p.I27L (rs1169288) variation had not only reflected the B cell disability, but also played a distinct role in the pathogenesis of insulin resistance [5-6]. Holmkvist *et al* have then confirmed that the I27L variation was related to increasing risk of type 2 diabetes with odds ratio of 1.5 [7-8]. Thus, the studies focusing on the sensing technics for I27L have been put on the agenda for early diagnosis of the disease to prevent possible complications; and also helpful for understanding the disease pathogenesis or for evaluating the pharmacological efficiency of therapeutic drugs [9].

Recently, there has been a great interest in developing various DNA biosensors to monitor the DNA hybridization, based on the signaling of radiochemistry, enzymatic catalysis, fluorescence, optical or acoustic techniques *etc* [10-13]. They have achieved high sensitivity and selectivity, but still face some imperfect issues as the requirement of tedious labels, costly polymerase, time consuming / complex

operation, or expensive instrumentation [14-16]. Therefore, more effective and accurate techniques for specific DNA assay are still in expectation. The electrochemiluminescence (ECL), a promising approach with admirable versatility, high sensitivity, good controllability, simple operation and installation, has attracted considerable attention [17-21]. Up to now, the ECL sensing has been attempted in DNA analysis owing to these merits [22-26].

Nano-sized metal materials have attracted considerable interest for their large surface area, good conductivity, striking catalytic activity and good biocompatibility [27, 28]. Among them, the gold nano-particles (AuNPs) is an outstanding one and easiest for mass-production (MP) with uniform performance. It ensures a strong interaction with biomolecules via Au-N or Au-S bonds or electrostatic interaction [29-31] to immobilize biomaterials without the loss of their bioactivity. It has already been demonstrated to be useful in the construction of those electrochemical sensors or biosensors as “electron antennae” to efficiently channel the electrons [32–34]. Thus, it is utilized as an intermediator to immobilize biomaterials to build high performance electrochemical biosensors [35], including DNA biosensors [36-39]. However, how to control the size, monodisperse, morphology, surface chemistry and the assembly of AuNPs on electrode surface is still a great challenge for its real application [40, 41].

In this work, with indium tin oxide (ITO) glass as the conductive substrate, the AuNPs have been assembled on its surface via the adhesion of hydrolyzed polymer of (3-aminopropyl) trimethoxysilane (APTMS) to prepare the Au plate electrode with nano-characteristic. After optimized all of the parameters, the electrode exhibits excellent electrochemical activity and catalysis. Thereafter, a novel label-free genetic biosensor was built up for rapid qualitative and quantitative discrimination of I27L mutation. Here the AuNPs/ITO base electrode was obtained by a simple two-steps

drip-coating procedure and the single-stranded oligonucleotide as capture probe (CP) was immobilized via Au-S bond directly. By using the quenched ECL of luminol as indicator, the hybridization between probe and target strand (TS) can be assessed. Originally, the sensor response is triggered by transfer dynamics of ECL probe but not any chemical reaction. This new mechanism is beneficial for more sensitive, stable and reproducible sensing performance. And meanwhile the preparation of proposed sensor is easily operated, low cost, excellent reproducible and has great potential for industrial MP, which meets the need of clinical usage as disposable device and especially for point-of-care test (POCT).

2. Experimental

2. 1 Reagents and materials

All oligonucleotides (including capture probe, CP; target strand, TS; 1-base mismatched target strand, 1MT; 3-base mismatched target strand, 3MT and noncomplementary sequence, NC, listed in Table 1) were synthesized and purified by high performance liquid chromatography (HPLC) by Shanghai Sangon Biotech Co., Ltd. (Shanghai, P. R. China). The ITO glass (from Nippon Sheet Glass Electronics Co., Suzhou, P. R. China), cut into 1.0 cm × 5.0 cm pieces, are used as working electrode (with 0.5 cm^2 of effective electrode area). Luminol was purchased from Fluka (USA). Tris (2-carboxyethyl) phosphine hydrochloride (TCEP) were from Shanghai Macklin Biochemical Co., Ltd (Shanghai, P. R. China). 3-aminopropyltrimethoxysilane (APTMS) and tris (hydroxymethyl) aminomethane (Tris-HCl) were purchased from Aladdin Industrial Co., Ltd. (Shanghai, P. R. China). All of other chemicals were obtained from Sinopharm Chemical Reagent Co., Ltd. (Shanghai, P. R. China). All chemicals are of analytical grade and used as received without further purification. Ultrapure water is obtained from an ALH-6000-U water

purification system (Aquapro, P. R. China). The buffers and solutions involved in this work are: Immobilization buffer (I-buffer; 10 mM Tris-HCl, 1 mM EDTA, 500 mM NaCl, 10 mM TCEP, pH=8.0), Hybridization buffer (H-buffer; 10 mM Tris-HCl, 1 mM EDTA, 500 mM NaCl, 1 mM $MgCl_2$, pH=8.0), ECL buffer (E-buffer; 0.02 M phosphate buffer solution (PBS), 5×10^{-8} M luminol, pH=8.0).

Table 1 should be placed here

2. 2 Instruments

The ECL experiments were carried out on our lab-built installation as reported in previous paper [42]. The measurements of electrochemical impedance spectroscopy (EIS) and cyclic voltammetry (CV) were performed on an RST-5200 Electrochemical Workstation (Risetest Instruments Co. Ltd., Suzhou, P. R. China). Scanning electron microscope (SEM) (S-4700 scanning electron microanalyzer, Hitachi, Japan) and transmission electron microscope (TEM) (FEI, USA, at an accelerating voltage of 200 KV) were used to observe the size and morphology of nanomaterials.

2. 3 Preparation of the AuNPs

AuNPs were prepared according to the literature [43]. Briefly, under vigorously magnetic stirring and heated to 100 ^{o}C, 4.5 mL of 1 % sodium citrate solution was added into 100 mL of 0.01 % $HAuCl_4$ solution, and allowed the reaction until the color of solution changed to wine red. The obtained AuNPs colloid was centrifuged at 3000 rpm for 10 min to eliminate those larger or agglomerated AuNPs. Thereafter, 3.5 mL of the supernatant was centrifuged again at 10,000 rpm for 30 min to condense the AuNPs by discarding supernatant liquid, and then the concentrate was re-dispersed with water to 250 μL.

2. 4 Fabrication of the genetic sensor

The fabrication process of the genetic biosensor is shown in Scheme 1. In order to enhance the electron transfer and to improve the biocompatibility, a functional layer of AuNPs was deposited on the surface of ITO glass ("a" to "c" in Scheme 1). At first, a flake of ITO was ultrasonically washed with 1:1 (v/v) ethanol / NaOH (1 M) mixture, acetone, ultrapure water (20 min each) in sequence, then immersed in 30% $NH_3 \cdot H_2O$ for 12 h to acquire a hydrophilic surface with dense -OH groups. Thereafter, the APTMS solution (0.01 % of anhydrous ethanol, v/v) was scattered on it. After the volatilization of ethanol in an equilibrium environment with saturated ethanol vapor, the ITO flake was transferred into a hygrothermostat to ensure the complete its hydrolysis (at 25 °C, for about 1 hour). Then, this flake was thoroughly flushed with ethanol to remove physically adsorbed APTMS, and dried with nitrogen stream. Subsequently, 50 μL of condensed AuNPs dispersion was dropped onto its surface in quiescence in 4 °C refrigerator for a period of 2.5 h to deposit the AuNPs. At last, it was rinsed with water and dried with nitrogen blowing.

Scheme 1 should be placed here

In order to prepare AuNPs/ITO electrode with good performance, a Taguchi orthogonal array $L_{16}(4^3)$ (three parameters, four levels) was designed for optimization of important parameters including the concentration of APTMS, amount of AuNPs and the length of period, as listed in Table 2A.

The step "d" in Scheme 1 illustrates the process of capture probe immobilization. 10 μL of I-buffer solution containing 5 μM of the thiolated CP was dropped onto the AuNPs/ITO electrode, and incubated for 4 h at 35 ^{o}C. During this period, the CP are

covalently linked onto the surface of the AuNPs/ITO via Au-S binding with thiol groups at 5'end of strand. It was then rinsed with PBS (5 mM) to remove adsorbed strands and dried in nitrogen atmosphere.

2. 5 The course of ECL sensing

The ECL detection was performed in a homemade ECL cell, and a conventional three-electrode system was used including an Ag wire as reference electrode, a platinum wire as auxiliary electrode. When a pulsed electrolytic potential was exerted on the sensor, the ECL signal of luminol was generated and recorded (step "e" in Scheme 1). Afterward, 10 μL of H-buffer containing TS or MTs was pipetted onto the sensor surface, incubated for 2 h at 35°C to ensure their hybridization with CP, and rinsed/dried. With the ECL emission of luminol on CP/AuNPs/ITO as background signal (the inserted B in Scheme 1), the delta of ECL intensity (ΔI) was recorded as the sensing signal.

3. Results and discussion

3. 1 The optimization of the conditions for sensor

The AuNPs functionalized substrate electrode is the critical role in sensor construction to ensure its high performance. By the analysis upon the results of orthogonal experiment (see Fig. 1) with designed parameters as listed in Table 2A, the fabrication conditions of this substrate electrode were optimized. Within the scopes of those parameters, the ECL intensity varied from 0.499 to 2.50 (see Table 2B), thus the $A_2B_3C_2$ was decided as the best acceptable option for optimal ECL behavior (C_{APTMS} = 0.05% (v/v), t = 2.5 h, $n_{AuNP} = 1.7\times10^{-6}$ moles).

Table 2 should be placed here

Fig. 1 should be placed here

Here the time-consumption of the steps “b” and “c” are both temperature dependent. The experimental results indicated, the step durations can be shortened to less than half-hour if heating-up to 55 °C for step “b” or 25 °C for step “c”. But, considering better reproducibility of this substrate electrode, we prefer to control the temperature at 25 °C and 4 °C, respectively, to ensure a slower but reproducible procedure.

Thereafter, the merits of sensing output of resultant biosensor is dependent upon the immobilization of CP on abovementioned substrate electrode. The conditions for self-assembling of CP are all required to be optimized including the CP concentration, temperature and duration. Fig. 2A reveals that the ECL intensity dropped drastically with the increasing concentration of CP and then remained steady at 5 μM, indicating a saturated bonding of CP on AuNPs/ITO electrode. Subsequently, the influences of temperature and time for self-assembly were also examined, as shown in Fig. 2B and 2C. It is closely related to the temperature, reached to maximum at 35 ^{o}C, and a period of 4 h is sufficient.

Fig. 2 should be placed here

Under these optimized conditions, the sensor was prepared successfully. Fig. 3 displays the SEM images of bare ITO (Fig. 3A), AuNPs/ITO (Fig. 3B), and the resultant sensor (Fig. 3C) respectively. It shows that an orderly and uniform AuNPs (the TEM image of AuNPs is displayed as the insert in Fig. 3B, with the size of 16 ± 2 nm) monolayer was dispersed on the surface of ITO by the adhesion of hydrolyzed

APTMS. Fig. 3C shows that the CP was evenly coated on the surface of AuNPs, resulted in some degree of agglomeration of those AuNPs.

The conditions for sensing implement were also optimized as: 35°C of temperature (Fig. 2D) and 2 h of time (Fig. 2E) for hybridization between CP and TS. By the comparison between the SEM images C and D in Fig. 3, it makes clear there were denser adherends (ds-DNA, image D) on the sensor surface, indicating the successfully hybridization of TS on CP.

Fig. 3 should be placed here

3. 2 The electrochemical investigation of AuNPs decoration

In 0.1 M KCl solution containing 5 mM $Fe(CN)_6^{3-}$, at the scan rate of 50 $mV \cdot s^{-1}$, the bare ITO showed a couple of well-defined reversible redox peak of $Fe(CN)_6^{3-}$ on cyclic voltammogram (CV) (curve a in Fig. 4A). When APTMS was applied on, however, the decrement of peak current was observed (curve b in Fig. 4A) because of the obstruction of those nonconductive macromolecules for electron transfer. Following the decoration of AuNPs, the peak current (curve c in Fig. 4A) obviously improved (greater than bare ITO), indicating an excellent function of AuNPs for offering an electron transfer channel for redox of $Fe(CN)_6^{3-}$. Meanwhile, the EIS could provide further information on the impedance changes of electrode surface during the process. In EIS, the electron-transfer resistance (R_{et}), which is represented by a diameter of the semicircle in the Nyquist plot, is the most directive and sensitive parameter responding to the changes of electrode interface. In Fig. 4B, the R_{et} increased when APTMS film was covered on bare ITO (see curves a and b). However, a much smaller R_{et} was observed (curve c), following by the decoration of AuNPs on

the electrode, indicating that AuNPs effectively accelerated the electron transfer. Fig. 4C exhibits the CVs of various electrodes in a PBS solution containing 2.5×10^{-5} M luminol. As we can see, compared with bare ITO (curve a) and APTMS/ITO (curve b), the peak currents highly increased on AuNPs decorated electrode (curve c), demonstrating the excellent feature of AuNPs for the oxidation of luminol. Furthermore, as displayed in Fig 4D, a very clear oxidation peak of luminol emerged at the potential of about 0.45 V on AuNPs decorated electrode (curve a), other than nothing on bulk Au electrode (curve b). It manifested that the AuNPs greatly facilitated the electron transfer of luminol to electrode, which increased its oxidizing rate. These results have clearly demonstrated the high performance of AuNPs/ITO to act as an excellent sensing platform.

Fig. 4 should be placed here

3. 3 ECL quenching mechanism of the sensor

To clarify the quenching mechanism of this sensor, the characteristics of the immobilization and hybridization of DNA were studied by CV and EIS with $Fe(CN)_6^{3-}$ as probe. As can be seen in Fig. 4A and 4B, when the CP was immobilized on the AuNPs/ITO, the redox peak current of probe decreased obviously and the R_{et} value increased greatly. These results can be introduced to confirm the electrostatic repulsion of negatively charged CP toward $Fe(CN)_6^{3-}$ and blocked electrode surface by the CP. Then the specific interaction of TS on CP will further boost it, similar as the description in references [44-47].

In order to further clarify the ECL quenching mechanism of this sensor, with luminol as probe, the CVs in PBS solution (Fig. 4C) demonstrated the decreased

redox currents when CP was assembled on AuNPs/ITO and further hybridization with TS.

These results have made it clear that the ECL signal of luminol is quenched by two main forces (see Scheme 1). Firstly, the electrostatic repulsion is one of them. The phosphate groups in backbone of DNA strand have been negatively charged because of hydrolysis at pH 8.0 [48], meanwhile the molecules of luminol forms a negatively charged anion (Lum^-) by deprotonation in this condition [49]. Thus there must be electrostatic repulsion between them. So the resultant sensor will repel the Lum^- probe to result in descending luminescence. The second factor is the space resistance. As shown in Scheme 1, as biological macromolecules, DNA has a large space steric hindrance that baffled the Lum^- probe to approach the electrode surface. These two forces hindered the Lum^- transfer to the electrode surface, so the route of forming exciting state of luminol (Lum*) was blocked to induce the quenched ECL signal.

3. 4 The optimization of ECL detecting conditions

The potential and period of pulsed electrolytic power play important roles in ECL analysis. Fig. 5A reveals the optimal pulse period of 3 s. Fig. 5(B, C) illustrate the ECL intensity dependent upon the limiting potentials of the pulse. It is clear that the highest ECL response was obtained at -0.3 V of lower limiting potential and 1.2 V of upper limiting potential. In addition, buffered pH of supporting solution on the sensing output was also studied (Fig. 5D). The optimal pH for the biosensor response should be a compromised result between the activity of oligonucleotides and the luminous behavior of luminol. A condition of pH 8.0 is the best choice. Under these optimized conditions, the ECL signal of electrodes are displayed in Fig. 5E. Obviously, the AuNPs functionalized electrodes (c) exhibited 27-fold higher ECL

signal than bare ITO (a), and even greater than APTMS/ITO (b). Although the sulfhydryl is easily oxidized to form the disulfide through S-S bonding at the potential about 0.7 V, it is clear that the immobilized CP on electrode surface was stable enough (d, give a RSD of less than 1%) owing to the CP was captured by AuNPs via Au-S bond, there are no -SH anymore. Also the output of the sensor responding to TS (e) is still stable enough. This electrode also exhibited excellent reproducibility. The relative standard deviation (RSD) for seven electrodes was 3.2 %.

Fig. 5 should be placed here

3. 5 The sensing performance of resultant sensor

The sensitivity of the sensor was assessed by monitoring the ECL response at different concentration of TS under optimal conditions. Fig. 6A exhibits the real maps of ECL emission on sensor at different TS concentrations. It could be found that the decreased ECL intensity was related to the concentration of TS. Fig. 6B shows that the responding signals increased along with the rise of TS concentration from 0 to 10 μM. The inset in Fig. 6B demonstrates that the responding signals of the sensor exhibited a linear correlation to the logarithm of TS concentration ranged from 0.01 nM to 10 μM with an equation of $\Delta ECL = 2.15 + 0.19 \lg C$ (M) ($R = 0.994$, $S_D = 0.029$) and a detection limit of 8.1×10^{-12} M (S/N=3).

Fig. 6 should be placed here

By comparison with other reported DNA biosensors as listed in Table 3, the resultant ECL sensor shows a lower detection limit and wider dynamic detection range for the target DNA assay.

Table 3 should be placed here

To evaluate the specificity of the sensor, four different sequenced oligonucleotides were chosen for investigation, including TS, single-base mismatched target (1MT), three-base mismatched target (3MT), and totally noncomplementary sequence (NC). The response signals of the blank sample or these four strands are showed in Fig. 7A. From it we can see significantly different responses within those sequences, here the quenched ECL signal of TS is obviously larger than that of 1MT, 3MT, and NC. In addition, CV and EIS were also used to further verify it. The peak current of NC, 3MT, 1MT and TS gradually decreased (curves a to e in Fig. 7B), the R_{et} of NC, 3MT, 1MT and TS gradually increased (curves a to e in Fig. 7C), entirely consisted with the result of ECL. The results demonstrate that the resultant sensor has selective recognizing ability for TS from NC, 3MT and 1MT. By this means, it might be expectable to effectively discriminate different DNA sequences.

Fig. 7 should be placed here

Meanwhile, Fig. 7D, after a 15 days period, displays about 92 % of remained response of its initial value, stored in PBS at 4 ^{o}C when not in use, implying a satisfactory long-term stability. The reproducibility of the sensor was investigated by

detection of a 1.0×10^{-8} M TS solution using five parallel sensors. The RSD was 3.4%, implying that the proposed sensor is reliable.

Conclusion

This work has designed a new and simple biosensor for rapid recognition and quantification of genic segment by employing AuNPs to functionalize the substrate electrode and load the capture oligonucleotide. This biosensor works in label-free manner, requires no labeling process. Under the optimal conditions, the quenched ECL intensity linearly relates to the logarithm of the target concentration from 1.0×10^{-11} to 1.0×10^{-7} M, with a detection limit of 8.1×10^{-12} M. The sensor has the ability to discriminate the diabetes related I27L genetic sequence from even single-base mismatched strand. This sensor is suitable for disposable use as in point-of-care testing and can be easily transformed for other genic sensing by immobilizing other probing strand. To fully assess the potential application and to reflect its value, future research will focus on integrating it with PCR technique for detection of I27L gene mutations in real patient samples, such as the samples extracted from cells, or hyphenating to separation systems as chromatography or electrophoresis.

Acknowledgments

This work is financially supported by the National Natural Science Foundation of China (21375091, 21675115).

References

[1] R. B. Prasad, L. Groop, Genetics of type 2 diabetes-pitfalls and possibilities, Genes, 6(2015), pp. 87-123.

[2] Diabetes Atlas, 2015. Available online: http://www.idf.org/diabetesatlas (accessed on 3 June 2016).

[3] World Health Organization. WHO report. 2015. Available online: http://www.who.int/gho/publications/en/ (accessed on 6 June 2016).

[4] M. Prabhanjan, R. V. Suresh, M. N. Murthy, N. B. Ramachandra, Type 2 diabetes mellitus disease risk genes identified by genome wide copy number variation scan in normal populations, Diabetes Res. Clin. Pract., 113(2016), pp. 160-170.

[5] K. C. Chiu, L. M. Chuang, J. M. Ryu, G. P. Tsai, M. F. Saad, The I27L amino acid polymorphism of hepatic nuclear factor-1α is associated with insulin resistance, J. Clin. Endocrinol. Metab., 85(2000), pp. 2178-2183.

[6] K. C. Chiu, L. M. Chuang, A. Chu, C. Yoon, M. Wang, Comparison of the impact of the I27L polymorphism of the hepatocyte nuclear factor-1alpha on estimated and measured beta cell indices, Eur. J. Endocrinol., 148(2003), pp. 641-647.

[7] J. Holmkvist, C. Cervin, V. Lyssenko, W. Winckler, D. Anevski, C. Cilio, C. M. Lindgren, Common variants in HNF-1 α and risk of type 2 diabetes, Diabetologia, 49(2006), pp. 2882-2891.

[8] J. Holmkvist, P. Almgren, V. Lyssenko, C. M. Lindgren, K. F. Eriksson, B. Isomaa, L. Groop, Common variants in maturity-onset diabetes of the young genes and future risk of type 2 diabetes, Diabetes, 57(2008), pp. 1738-1744.

[9] K. E. North, N. Franceschini, C. L. Avery, L. Baird, M. Graff, M. Leppert, K. A. Volcik, Variation in the checkpoint kinase 2 gene is associated with type 2 diabetes in multiple populations, Acta Diabetol., 47(2010), pp. 199-207.

[10] G. Papadakis, A. Tsortos, A. Kordas, I. Tiniakou, E. Morou, J. Vontas, E. Gizeli, Acoustic detection of DNA conformation in genetic assays combined with

PCR, Sci. Rep., 3(2013), 2033. Available on line: http://www.nature.com/articles/srep02033.

[11] N. Dai, E. T. Kool, Fluorescent DNA-based enzyme sensors, Chem. Soc. Rev., 40 (2011), pp. 5756-5770.

[12] H. Meng, Y. Yang, Y. Chen, Y. Zhou, Y. Liu, X. A. Chen, L. Jiang, Photoelectric conversion switch based on quantum dots with i-motif DNA scaffolds, Chem. Commun., 17(2009), pp. 2293-2295.

[13] Z. Li, Z. Zhu, W. Liu, Y. Zhou, B. Han, Y. Gao, Z. Tang, Reversible plasmonic circular dichroism of Au nanorod and DNA assemblies, J. Am. Chem. Soc., 134 (2012), pp. 3322-3325.

[14] V. T. Tran, H. Zhou, S. Kim, J. Lee, J. Kim, F. Zou, J. Kim, J. Y. Park, J. Lee, Self-assembled magnetoplasmonic nanochain for DNA sensing, Sens. Actuators B: Chem., 203(2014), pp. 817-823.

[15] X. Chen, C. Y. Hong, Y. H. Lin, J. H. Chen, G. N. Chen, H. H. Yang, Enzyme-free and label-free ultrasensitive electrochemical detection of human immunodeficiency virus DNA in biological samples based on long-range self-assembled DNA nanostructures, Anal. Chem., 84(2012), pp. 8277-8283.

[16] H. Huang, W. Bai, C. Dong, R. Guo, Z. Liu, An ultrasensitive electrochemical DNA biosensor based on graphene/Au nanorod/polythionine for human papillomavirus DNA detection, Biosens. Bioelectron., 68(2015), pp. 442-446.

[17] X. Zheng, Z. Guo, Z. Zhang, Flow-injection electrogenerated chemiluminescence determination of epinephrine using luminal, Anal. Chim. Acta, 441(2001), pp. 81-86.

[18] A. Arora, J. C. Eijkel, W. E. Morf, A. Manz, A wireless electrochemiluminescence detector applied to direct and indirect detection for

electrophoresis on a microfabricated glass device, Anal. Chem., 73(2001), pp. 3282-3288.

[19] A. Chovin, P. Garrigue, N. Sojic, Electrochemiluminescent detection of hydrogen peroxide with an imaging sensor array, Electrochim. Acta, 49(2004), pp. 3751-3757.

[20] L. Hu, G. Xu, Applications and trends in electrochemiluminescence, Chem. Soc. Rev., 39(2010), pp. 3275-3304.

[21] E. J. O'Reilly, T. E. Keyes, R. J. Forster, L. Dennany, Insights into electrochemiluminescent enhancement through electrode surface modification, Analyst, 138(2013), pp. 677-682.

[22] M. Li, Y. Wang, Y. Zhang, J. Yu, S. Ge, M. Yan, Graphene functionalized porous au-paper based electrochemiluminescence device for detection of DNA using luminescent silver nanoparticles coated calcium carbonate/carboxymethyl chitosan hybrid microspheres as labels, Biosens. Bioelectron., 59(2014), pp. 307-313.

[23] Y. Feng, Q. Wang, J. Lei, H. Ju, Electrochemiluminescent DNA sensing using carbon nitride nanosheets as emitter for loading of hemin labeled single-stranded DNA, Biosens. Bioelectron., 73(2015), pp. 7-12.

[24] X. Hu, R. Wang, Y. Ding, X. Zhang, W. Jin, Electrochemiluminescence of CdTe quantum dots as labels at nanoporous gold leaf electrodes for ultrasensitive DNA analysis, Talanta, 80(2010), pp. 1737-1743.

[25] L. Shen, J. Li, L. Li, G. Zou, X. Zhang, W. Jin, Ultrasensitive electrochemiluminescence method for determination of DNA using $Ru(bpy)_3^{2+}$ coated magnetic submicrobeads wrapped with carbon nanotubes, Electrochem. Commun., 13(2011), pp. 1499-1501.

[26] R. Duan, X. Zhou, D. Xing, Electrochemiluminescence biobarcode method based on cysteamine-gold nanoparticle conjugates, Anal. Chem., 82(2010), pp. 3099-3103.

[27] X. Liu, J. Zhang, S. Liu, Q. Zhang, X. Liu, D.K. Wong, Gold nanoparticle encapsulated-tubular TiO2 nanocluster as a scaffold for development of thiolated enzyme biosensors, Anal. Chem., 85(2013), pp. 4350-4356.

[28] G. K. Ahirwal, C. K. Mitra, Gold nanoparticles based sandwich electrochemical immunosensor, Biosens. Bioelectron., 25(2010), pp. 2016-2020.

[29] H. Tang, J. Chen, L. Nie, Y. Kuang, S. Yao, A label-free electrochemical immunoassay for carcinoembryonic antigen (CEA) based on gold nanoparticles (AuNPs) and nonconductive polymer film, Biosens. Bioelectron., 22(2007), pp. 1061-1067.

[30] Y. Zhang, L. Huang, Label-free electrochemical DNA biosensor based on a glassy carbon electrode modified with gold nanoparticles, polythionine, and grapheme, Microchim. Acta, 176(2012), pp. 463-470.

[31] J. Lu, S. Liu, S. Ge, M. Yan, J. Yu, X. Hu, Ultrasensitive electrochemical immunosensor based on Au nanoparticles dotted carbon nanotube-graphene composite and functionalized mesoporous materials, Biosens. Bioelectron., 33 (2012), pp. 29-35.

[32] M. C. Daniel, D. Astruc, Gold nanoparticles: assembly, supramolecular chemistry, quantum-size-related properties, and applications toward biology, catalysis, and nanotechnology, Chem Rev., 104(2004), pp. 293-346.

[33] C. R. Raj, T. Okajima, T. Ohsaka, Gold nanoparticle arrays for the voltammetric sensing of dopamine, J. Electroanal. Chem., 543(2003), pp. 127-133.

[34] K. R. Brown, A. P. Fox, M. J. Natan, Morphology-dependent electrochemistry of cytochrome C at Au colloid-modified SnO_2 electrodes, J. Am. Chem, Soc., 118(1996), pp.1154-1157.

[35] K. J. Huang, J. Li, Y. Y. Wu, Y. M. Liu, Amperometric immunobiosensor for α-fetoprotein using Au nanoparticles/chitosan/TiO_2-graphene composite based platform, Bioelectrochem., 90(2013), pp. 18-23.

[36] C. Z. Li, Y. Liu, J. H. Luong, Impedance sensing of DNA binding drugs using gold substrates modified with gold nanoparticles, Anal. Chem., 77(2005), pp. 478-485.

[37] D. Li, Y. Yan, A. Wieckowska, I. Willner, Amplified electrochemical detection of DNA through Au nanoparticles on electrodes and the incorporation into the DNA-crosslinked structure, Chem. Commun., 34(2007), pp. 3544-3546.

[38] W. J. Parak, T. Pellegrino, C. M. Micheel, D. Gerion, S. C. Williams, A. P. Alivisatos, Conformation of oligonucleotides attached to gold nanocrystals probed by gel electrophoresis, Nano Lett., 3(2003), pp. 33-36.

[39] X. R. Cheng, B. Y. Hau, T. Endo, K. Kerman, Au nanoparticle-modified DNA sensor based on simultaneous electrochemical impedance spectroscopy and localized surface plasmon resonance, Biosens. Bioelectron., 53(2014), pp. 513-518.

[40] S. Guo, E. Wang, Synthesis and electrochemical applications of gold nanoparticles, Anal. Chim. Acta, 598(2007), pp. 181-192.

[41] W. Ye, D. Wang, H. Zhang, F. Zhou, W. Liu, Electrochemical growth of flowerlike gold nanoparticles on polydopamine modified ITO glass for SERS application, Electrochim. Acta, 55(2010), pp. 2004-2009.

[42] Z. Yu, X. Wei, J. Yan, Y. Tu, Intensification of electrochemiluminescence of luminol on TiO_2 supported Au atomic cluster nano-hybrid modified electrode, Analyst, 137 (2012), pp. 1922-1929.

[43] A. Toyota, T. Sagara, Particle size dependence of the charging of Au nanoparticles immobilized on a modified ITO electrode, Electrochim. Acta, 53 (2008), pp. 2553-2559.

[44] R.K. Shervedani, S. Pourbeyram, A modification free hybridization biosensor for detection of DNA sequence based on Zr (IV) ion glue mediated the adsorption on Au-MPA SAM electrode, Sens. Actuators B: Chem., 160(2011), pp. 145-153.

[45] S. Deng, L. Cheng, J. Lei, Y. Cheng, Y. Huang, H. Ju, Label-free electrochemiluminescent detection of DNA by hybridization with a molecular beacon to form hemin/G-quadruplex architecture for signal inhibition, Nanoscale, 5(2013), pp. 5435-5441.

[46] G. Li, X. Li, J. Wan, S. Zhang, Dendrimers-based DNA biosensors for highly sensitive electrochemical detection of DNA hybridization using reporter probe DNA modified with Au nanoparticles, Biosens. Bioelectron., 24(2009), pp. 3281-3287.

[47] G. J. Li, L. H. Liu, X. W. Qi, Y. Q. Guo, W. Sun, X. L. Li, Development of a sensitive electrochemical DNA sensor by 4-aminothiophenol self-assembled on electrodeposited nanogold electrode coupled with Au nanoparticles labeled reporter ssDNA, Electrochim. Acta, 63(2012), pp. 312-317.

[48] Y. J. Ruan, J. Li, Analysis system of DNA gel electrophoresis, A dissertation for the professional degree of master of Harbin Engineering University, 2012. Available online:

(http://202.195.136.232/kcms/detail/detail.aspx?recid=&FileName=1012518296.nh&DbName=CMFDLAST2013&DbCode=CMFD&uid=anNQVVlZc25FT0FUTmU3K243TmR0S0xKY3AxMVBLaGhzZkFESzVKaUxYa2gzTlRu)

[49] J. R. An, X. Chen, H. Chen, Investigation of electrochemiluminescence of luminol in aqueous alkaline solution, Anal. Chem., 16(1988) pp. 127-132

[50] N. N. Zhu, A. P. Zhang, Q. J. Wang, P. G. He, Y. Z. Fang, Electrochemical detection of DNA hybridization using methylene blue and electro-deposited zirconia thin films on gold electrodes, Anal. Chim. Acta, 510(2004), pp. 163–168.

[51] K. J. Feng, Y. H. Yang, Z. J. Wang, J. H. Jiang, G. L.Shen, R. Q. Yu, A nano porous CeO 2/Chitosan composite film as the immobilization matrix for colorect al cancer DNA sequence-selective electrochemical biosensor, Talanta, 70(2006), pp. 561-565.

[52] P. M. Ndangili, R. A. Olowu, S. N. Mailu, R. F. Ngece, A. Jijana, A. Williams, Impedimetric response of a label-free genosensor prepared on a 3-mercaptopropionic acid capped gallium selenide nanocrystal modified gold electrode, Int. J. Electrochem. Sci, 6(2011), pp.1438-1453.

[53] N. Zhu, Z. Chang, P. He, Y. Fang, Electrochemical DNA biosensors based on platinum nanoparticles combined carbon nanotubes, Anal. Chim. Acta, 545(2005), pp. 21-26.

[54] R. K. Shervedani, S. Pourbeyram, A modification free hybridization biosensor for detection of DNA sequence based on Zr (IV) ion glue mediated the adsorption on Au–MPA SAM electrode, Sens. Actuators B: Chem., 160(2011), pp.145-153.

[55] X. Liu, X. Qu, H. Fan, S. Ai, R. Han, Electrochemical detection of DNA hybridization using a water-soluble branched polyethyleneimine–cobalt (III)–phenanthroline indicator and PNA probe on Au electrodes, Electrochim. Acta, 55(2010), pp. 6491-6495.

[56] J. Chen, J. Zhang, Q. Zhuang, J. Chen, X. Lin, Electrochemical studies of the interaction of 2‐nitroacridone with DNA and determination of DNA, Electroanalysis, 19(2007), pp. 1765-1772.

[57] H. Cai, X. Cao, Y. Jiang, P. He, Y. Fang, Carbon nanotube-enhanced electrochemical DNA biosensor for DNA hybridization detection, Anal. Bioanal. Chem., 375(2003), pp. 287-293.

Figure Captions

Scheme 1. Fabrication and detection process of the biosensor

Fig. 1 The results of orthogonal tests

Fig. 2 The effects of (A) the capture probe concentration; (B) the temperature for SAM; (C) the time of SAM; (D) the temperature for hybridization and (E) the time of hybridization on the ECL intensity of resultant sensor

Fig. 3 The SEM images of (A) ITO; (B) AuNPs/ITO, here the inserted one is the TEM image of AuNPs; (C) CP/AuNPs/ITO and (D) hybridized with TS

Fig. 4 The (A) CV (50 mV s^{-1} of scan rate) and (B) Nyquist plot of electrodes in 0.1 M KCl containing 5 mM $Fe(CN)_6^{3-}$. Electrodes from curve a to e are ITO, APTMS/ITO, AuNPs/ITO, resultant sensor and hybridized one, respectively. The insert in B is the equivalent circuit. (C) The CVs of 2.5×10^{-5} M luminol on (a) ITO, (b) APTMS/ITO, (c) AuNPs/ITO, (d) resultant sensor and (e) hybridized one in PBS (pH=8.0), 50 mV s^{-1} of scan rate; (D) The variation of redox performance of 2.5×10^{-5} M luminol on (a) AuNPs decorated ITO and (b) a commonly bulk Au electrode, CV with scan rate of 50 mV s^{-1} in PBS (pH=8.0)

Fig. 5 The effects of (A) pulse period and (B, C) lower/upper limiting potential on the ECL response of resultant biosensor toward TS, $C_{Luminol}=1\times10^{-7}$ M, pH=8.0; (D) The effects of pH on ECL response of resultant biosensor toward TS; (E) The ECL curves of (a) bare ITO, (b) APTMS/ITO, (c) AuNPs/ITO, (d) resultant biosensor and (e) the response toward TS in PBS (pH=8.0)

Fig. 6 (A) The ECL responses for different target strand concentrations, $C_{luminol}=5\times10^{-8}$ M, pH=8.0; (B) The relationship between the responding signals and TS concentration, the insert is the linear regression of responding signals upon logarithm of the target strand concentration

Fig. 7 (A) The ECL responses of the sensor upon different strands, including NC, 3MT, 1MT and TS, $C_{luminol}=5\times10^{-8}$ M, pH=8.0; The (B) CV and (C) Nyquist plot of (a) resultant sensor and to sense with 1.0×10^{-8} M of (b) NC, (c) 3MT, (d) 1MT or (e) TS, in 0.1 M KCl solution containing 5 mM $Fe(CN)_6^{3-}$

Table 1 The sequence of designed oligonucleotides used in this work

Oligonucleotides	Sequence (from 5′ to 3′)
capture probe (CP)	SH-$(CH_2)_6$-AAAGAGGCACTGCTCCAGGCACTGG
target strand (TS)	CCAGTGCCTGGAGCAGTGCCTCTTT
single-base mismatched target (1MT)	CCAGTGCCTGGA<u>T</u>CAGTGCCTCTTT
three-base mismatched target (3MT)	CCA<u>C</u>TGCCTGGA<u>T</u>CAGTGCCT<u>G</u>TTT
noncomplementary sequence (NC)	GGTCACGGACCTCGTCACGGAGAAA

* TS is completely complementary with CP. The underlined are the mismatched bases in 1MT or 3MT.

Table 2A The controlling factors and their levels of orthogonal test L_{16} (4^3)

Factors		Levels			
		1	2	3	4
A	C_{APTMS} / % (v/v)	0.01	0.05	0.1	0.15
B	t / h	0.5	1.5	2.5	12
C	n_{AuNPs} / mole	1.21×10^{-6}	1.70×10^{-6}	2.83×10^{-6}	8.50×10^{-6}

Table 2B The results of orthogonal test

Experiment NO.	Parameter and level			Results
	C_{APTMS} / %(v/v)	t / h	n_{AuNPs} / mole	ECL Intensity
1	0.0100	0.500	1.21×10^{-6}	0.50
2	0.0100	1.50	1.70×10^{-6}	0.95
3	0.0100	2.50	2.83×10^{-6}	1.52
4	0.0100	12.0	8.50×10^{-6}	1.69
5	0.0500	0.500	1.70×10^{-6}	2.50
6	0.0500	1.50	1.21×10^{-6}	1.83
7	0.0500	2.50	8.50×10^{-6}	2.46
8	0.0500	12.0	2.83×10^{-6}	2.27

9	0.100	0.500	2.83×10^{-6}	1.02
10	0.100	1.50	8.50×10^{-6}	0.90
11	0.100	2.50	1.21×10^{-6}	1.77
12	0.100	12.0	1.70×10^{-6}	1.63
13	0.150	0.500	8.50×10^{-6}	0.50
14	0.150	1.500	2.83×10^{-6}	1.10
15	0.150	2.50	1.70×10^{-6}	1.36
16	0.150	12.0	1.21×10^{-6}	1.21

Table 3 Comparison of linear ranges and detection limits of the different electrochemical DNA sensors.

Modified electrodes	Detection technique	Linear range (M)	Detection limit (M)	References
ZrO_2/Au	DPV	2.25×10^{-10}-2.25×10^{-8}	1.0×10^{-10}	[50]
CeO_2/CHIT/GC	DPV	1.59×10^{-11}-1.16×10^{-7}	1.0×10^{-11}	[51]
Ga_2Se_3/3MPA/Au	EIS	1.4×10^{-8}-2.0×10^{-8}	6.6×10^{-10}	[52]
MWCNTs/Pt_{nano}/GCE	DPV	2.25×10^{-11}-2.25×10^{-7}	1.0×10^{-11}	[53]
Au–MPA–Zr(IV)	EIS	1.0×10^{-10}-1.0×10^{-6}	8.5×10^{-11}	[54]
Au	DPV	5.0×10^{-9}-2.5×10^{-7}	5.6×10^{-10}	[55]
GCE	DPV	1.55×10^{-7}-2.02×10^{-6}	3.1×10^{-8}	[56]
4-ATP/NG/Au	DPV	1.4×10^{-11}-2.0×10^{-9}	9.5×10^{-12}	[47]
MWNTs–COOH/GCE	DPV	2.0×10^{-10}-5.0×10^{-8}	1.0×10^{-10}	[58]
AuNPs/ITO	ECL	1.0×10^{-11}–1.0×10^{-7}	8.1×10^{-12}	This study

Fig. 1

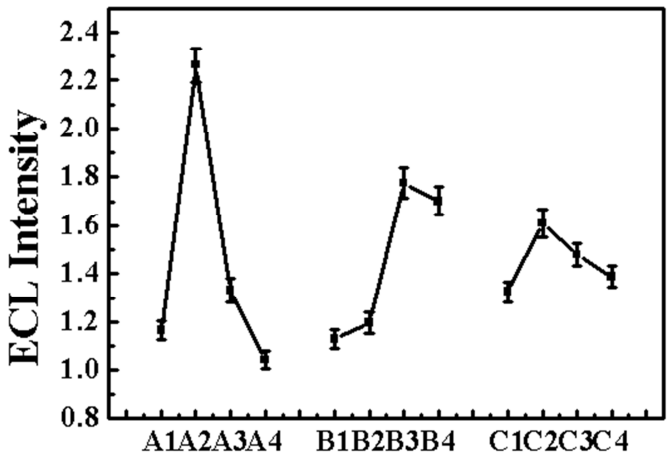

Fig. 2

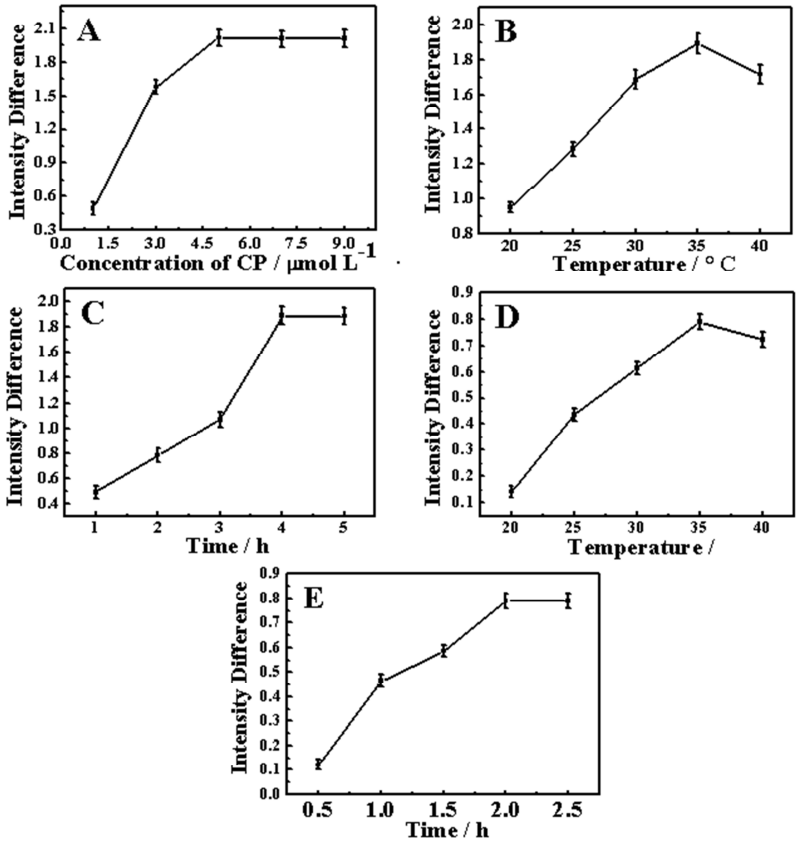

Fig. 3

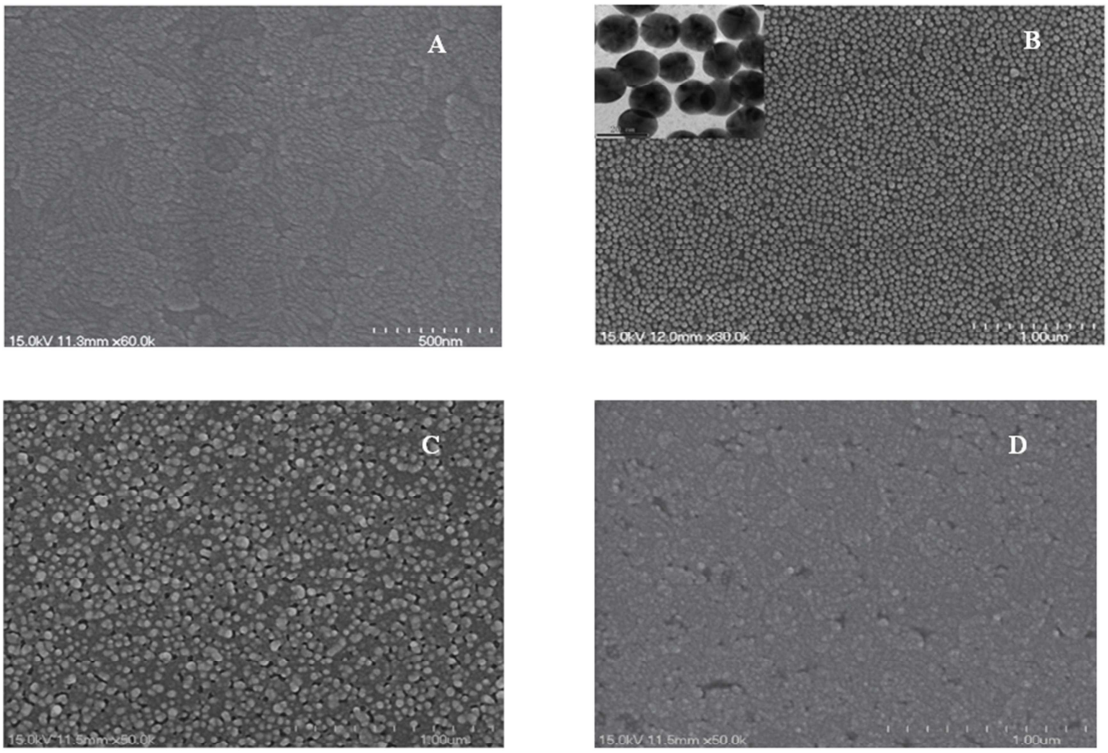

Fig. 4

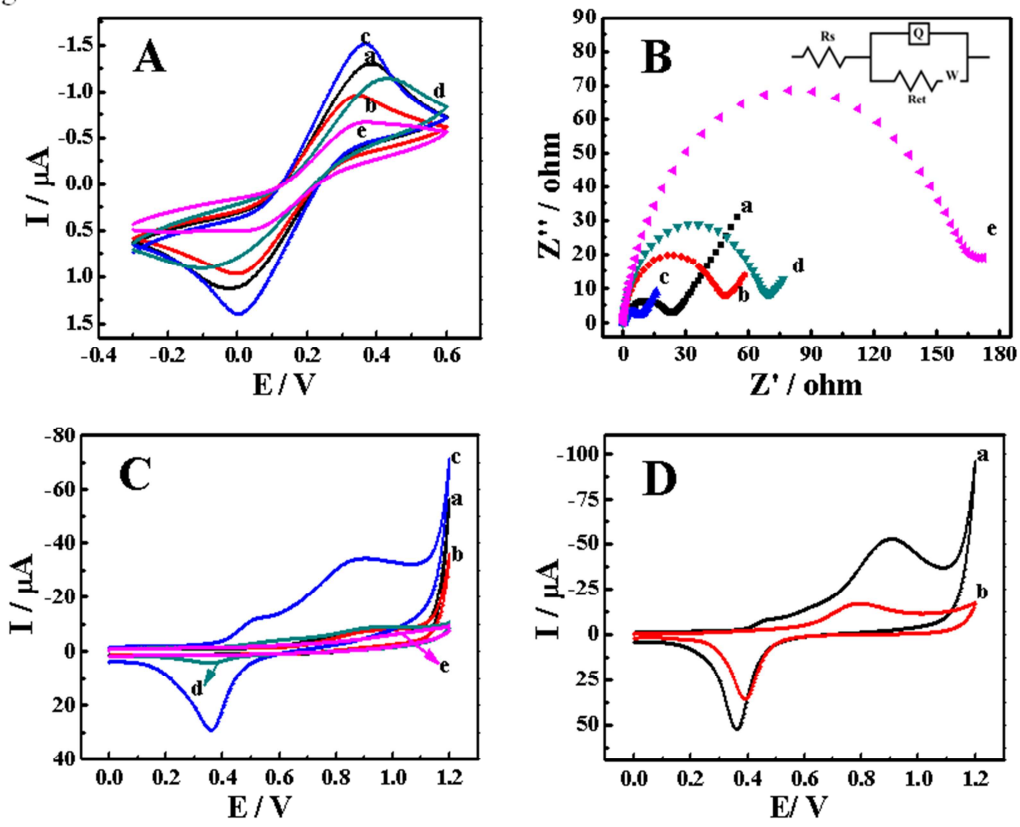

Fig. 5

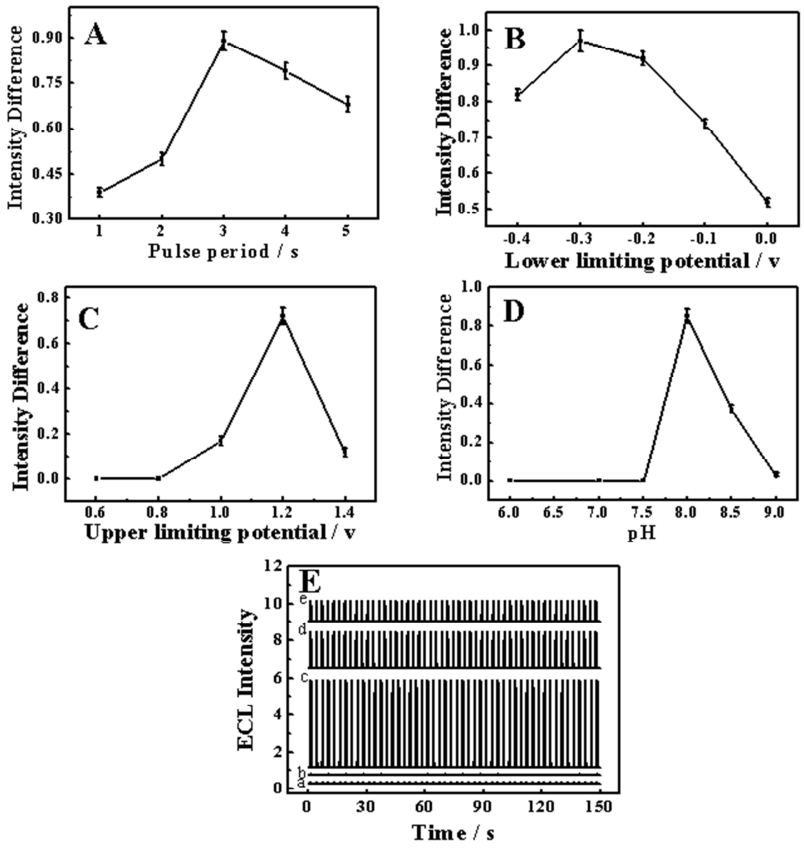

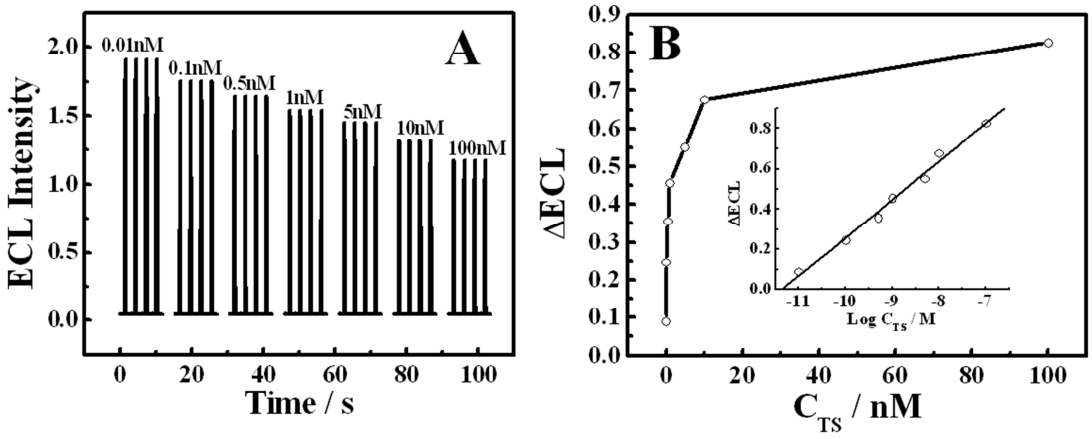

Fig. 7

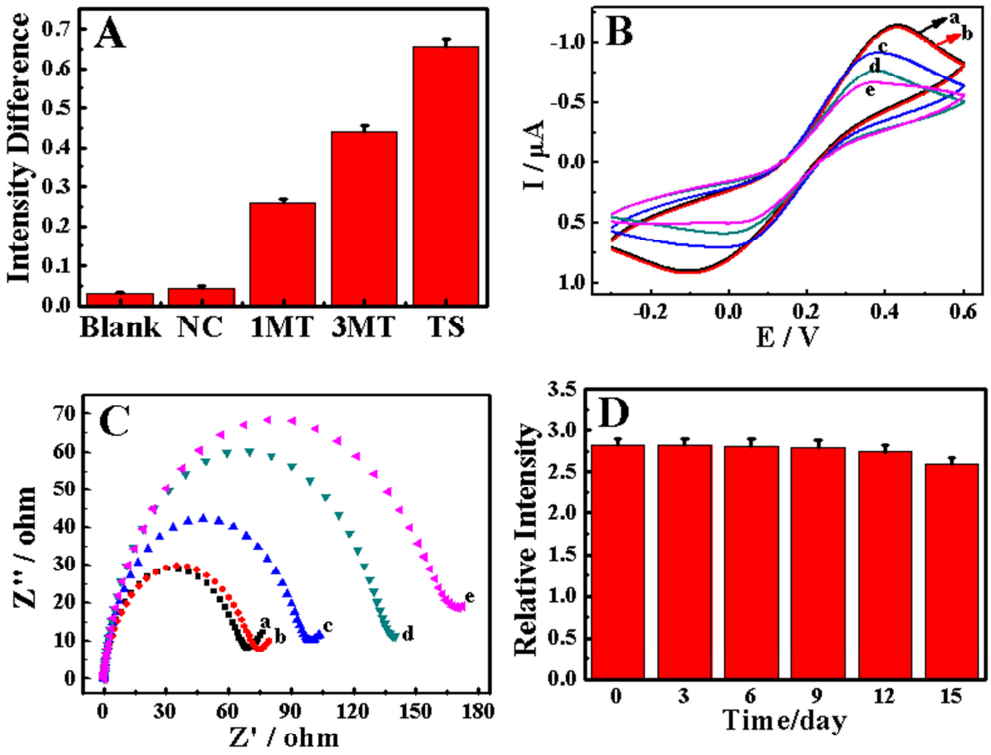

Scheme 1

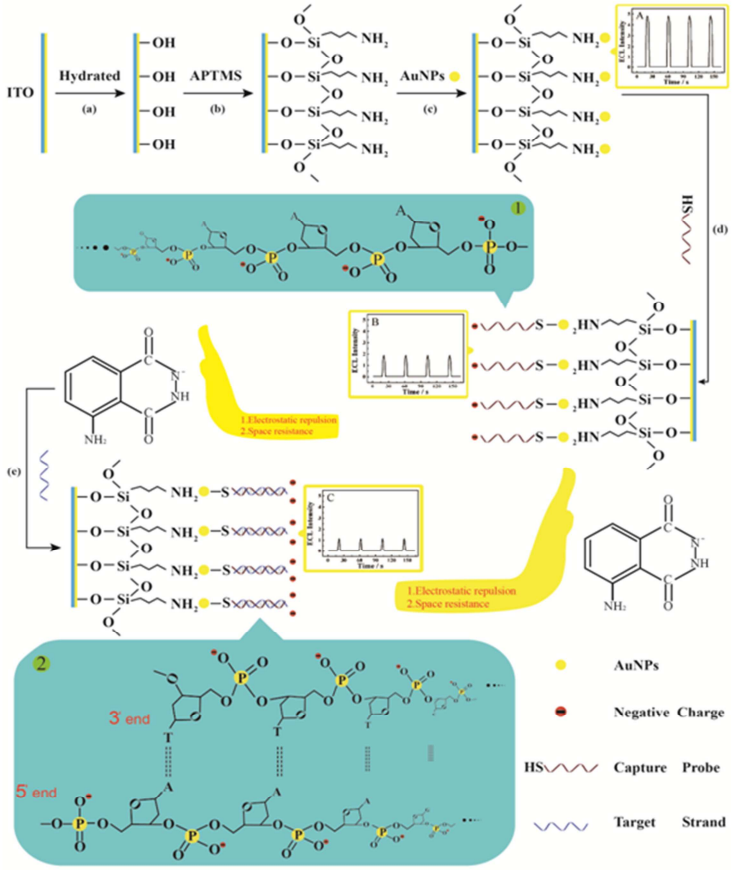

Research Highlight

► A label free biosensor for I27L gene variant (diabetes) with electrochemiluminescence of luminol as output signal

► The Au nanoparticles (AuNPs) decorated ITO acted as the substrate

► The biosensor exhibited high sensitivity, stability, excellent reproducibility and outstanding selectivity against mismatched DNA